

H14-201

UNDERSTANDING DISPERSION OF NANOPARTICLES IN VEHICLE WAKES COMBINING FIELD MEASUREMENTS AND WIND TUNNEL SIMULATIONS

Prashant Kumar^{1,2}, Matteo Carpentieri^{1,2}, Alan Robins², Matthias Ketzel³ and Rex Britter⁴

¹Division of Civil, Chemical and Environmental Engineering, Faculty of Engineering and Physical Sciences (FEPS), University of Surrey, GU2 7XH, UK

²Environmental Flow (EnFlo) Research Centre, Division of Mechanical, Medical and Aerospace Engineering, FEPS, University of Surrey, GU2 7XH, UK

³Department of Environmental Science, Aarhus University, DK-4000 Roskilde, Denmark

⁴Senseable City Laboratory, Massachusetts Institute of Technology, Boston, MA 02139, USA

Abstract: This work presents selected results of an EPSRC-funded project investigating the dispersion of nanoparticles in the wake of moving vehicles. The aims were to study the changes in particle number distribution (PND) due to the competing effects of dilution and transformation processes (e.g. coagulation, nucleation, condensation) over the travel time from tailpipe to roadside, and to model the fate of these particles in the near and the far wake regions of a moving vehicle. To achieve these objectives, firstly ground-fixed and on-board measurements of PNDs were performed using a fast response (sampling frequency up to 10Hz) differential mobility spectrometer (Cambustion DMS50) in the wake of a diesel engine car moving at a range of speeds from 20 to 50 km h⁻¹. Secondly, wind tunnel simulations were carried out on reduced scale (1:5 and 1:20) models of the car used for the field experiments. The flow and turbulence fields were characterised both in the near and far wake of the modelled vehicle by using a two component laser Doppler anemometer. Concentration measurements were obtained by using a fast response (frequency >350 Hz) flame ionisation detector and a hydrocarbon tracer gas released from the modelled tailpipe. A high resolution experimental data base was obtained from both the field and wind tunnel measurements for formulating the basis of fast mathematical parameterisations that can be used with operational nanoparticle dispersion models.

Key words: Number and size distribution; Ultrafine particle; Vehicle Wake; Nanoparticle dispersion; Wind tunnel; Dispersion model

INTRODUCTION

Road vehicles are the leading source of particles in the nanometre size range. They can enter the body through the skin, lung and gastrointestinal tract, leading to respiratory and cardiovascular diseases (Kumar et al., 2010). Just after the release of exhaust emissions, particle precursor gases undergo rapid transformation processes (i.e. nucleation, coagulation, condensation) that change the number and size distributions noticeably between the source (i.e. vehicle tailpipe) and the receptor (i.e. people travelling or living nearby the roads). A better understanding of these processes is essential for developing appropriate methods for including nanoparticle dynamics in dispersion models. Very short time scales are usually associated with nanoparticle transformations in the first stages after their emission, as highlighted by previous field measurements (Carpentieri and Kumar, 2011) and modelling studies (Carpentieri et al., 2011a; Kumar et al., 2011). The interaction between these transformations and the flow and turbulence fields immediately behind the vehicle is complex and strongly affect nanoparticle dispersion at local scale. However, this interaction has often been overlooked by past studies and it is therefore a need of characterising in detail the mixing processes in the vehicle wake and examining emissions from individual vehicles under real driving and dilution conditions. This work presents results of both a systematic wind tunnel experimental campaign and analogous field campaigns aimed at understanding nanoparticle dispersion in both the near and main/far wake regions of a diesel car running at different speeds.

MATERIALS AND METHODS

An instrument with a high sampling frequency is required to capture rapidly occurring transformation processes. In this work, a fast response differential mobility spectrometer (i.e. DMS50) was used to measure the number and size distributions in the 5–560 nm range with a sampling frequency of 10 Hz. Measurements were carried out in the wake of a diesel car (Vauxhall Astra Van; 1686 cm³ diesel engine; registered in 2004 under Euro 4 emission standards) which was run at 4 different speeds (i.e. $V = 20, 30, 40$ and 50 km h^{-1}). Two different sets of measurement using the same diesel car campaigns were carried out covering different heights in the wake regions: (i) ground-fixed (i.e. 0.10 and 0.25 m above the road surface at a lateral distance about $0.27 \pm 0.15 \text{ m}$ from the tailpipe exit), and (ii) on-board (i.e. at 12 different sampling locations behind the moving car). Locations of on-board measurements were at the centre, left/front of tailpipe, right, at three different vertical levels at 45 cm longitudinal distance from the back of the car. Three further measurement points were chosen at 0.80 m away from the rear body of the car for mapping the near wake region. On-board measurements were conducted using three different car speeds (20, 30 and 40 km h⁻¹). Meteorological data (wind speed and direction, temperature, pressure and humidity) were gathered from an on-site monitoring station as well as a fixed monitoring station about 250 m away from the experimental site. Both these experimental campaigns were conducted in the University of Surrey car park. Further details on the experimental set up can be seen in Carpentieri and Kumar (2011).

Wind tunnel experiments were carried out in the EnFlo (Environmental Flow Research Centre) facility at the University of Surrey. This is an open circuit suck-down tunnel with 20 m×3.5 m×1.5 m (length×breadth×height) working section and capable of handling 0.3 to 3.5 m s⁻¹ wind speed in both stable and unstable atmospheric conditions. Our experiments used 2.5 m s⁻¹ wind speed. Reduced scale models (1:20 and 1:5) of the diesel car used in our field experiments were deployed for measuring concentration, wind velocity and turbulence fields. While 1:5 model provided detailed flow characteristics in near wake, 1:20 model helped to capture data in the far wake region. For reducing the unrealistic effects of a growing boundary layer at the wind tunnel surface, the models were placed at the leading edge (at ~11 m from the inlet to the wind tunnel

working section) of a false floor (i.e. 0.23 m above the tunnel floor), which is a common practice for this kind of experiment (Kanda et al., 2006). This set up provided a nominal blockage factor for 1:5 and 1:20 models which was about 0.5 and 2.1%, respectively. The flow and turbulence fields were characterised both in the near and the far wake regions of the modelled vehicle by using a two component laser Doppler anemometer (LDA). The probe was used in two different positions (measuring velocity components both in the x–y, and x–z planes) in order to have a complete three-dimensional map. Concentration measurements were obtained by using a fast response (frequency >350 Hz) flame ionisation detector (FFID) and a hydrocarbon tracer gas (propane) released from the modelled tailpipe. Further description of the wind tunnel experiments can be seen in Carpentieri et al. (2011b).

RESULTS AND DISCUSSION

Ground-fixed and on-board measurements

Cross combination of total 8 experimental cases (i.e. height, $H = 0.10$ and 0.25 m, and car speeds, $V = 20, 30, 40$ and 50 km h^{-1}) made available a total of 65 valid experimental runs for data analysis. As anticipated from the field data, the variability and uncertainties associated with the different test cases (even in nominally identical conditions) were substantial. However, a number of common trends showing evolution of both particle number concentration (PNC) and distribution (PND) were observed. Figure 1 reports selection of the most commonly observed PNC patterns. This illustrates a rapid building of PNCs that peak normally within the first second (time, $t = 0$ being the time when the PNCs start increasing significantly from the background). This peak was followed by a rapid decay in next few seconds, and then a slightly slower decay, returning to background levels. As expected, the decay time for PNCs at both heights was found to be generally relatively longer for high car speeds (e.g. Figure 1b) compared with smaller car speeds (Figures 1a). This total effect lasted in most cases for just few seconds (i.e. ~ 5 – 15 s).

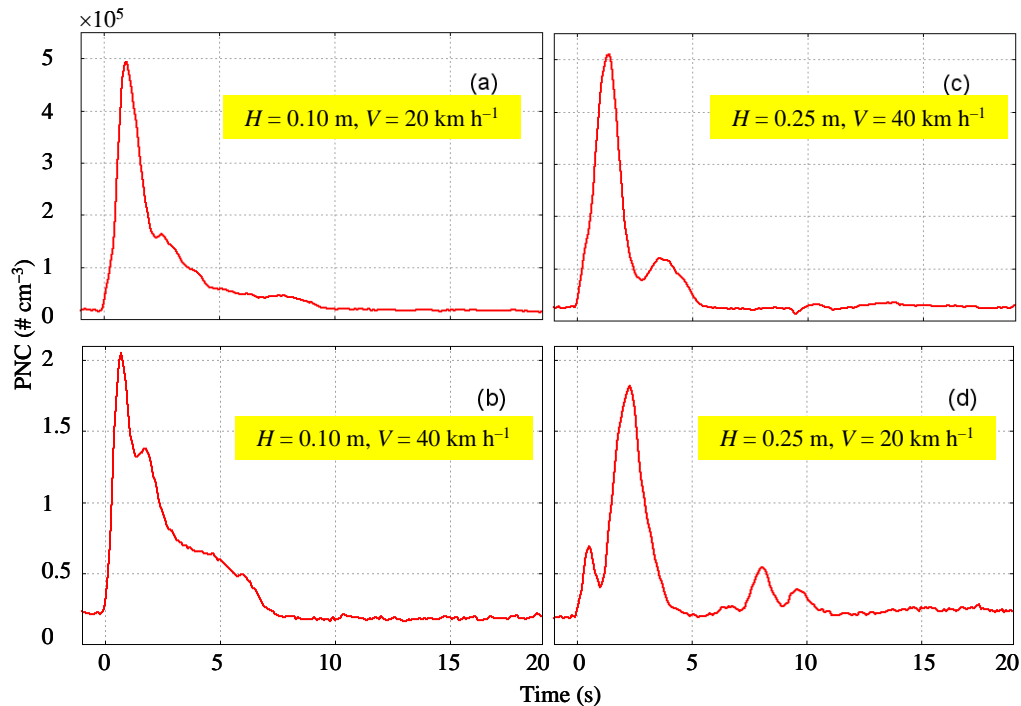


Figure 1. Typically observed variations in temporal evolution of PNCs for ground-fixed measurements during various experimental cases.

For further investigation, measured PND data were divided into three different temporal stages: (i) *pre-evolution*, where distributions can be considered as site background, (ii) *evolution*, which is of most interest due to rapidly occurring changes in particle number and size distributions, and (iii) *post-evolution*, the stage just after the evolution where distributions return back near to those found in pre-evolution stage. These results were consistent with our previous study (Kumar et al., 2009) where evolution stage completed in first few seconds, after which the background concentrations and distributions started establishing to those found in pre-evolution stage. The other most common pattern was an initial growth in PNC for the 40–90 nm size range, followed by a dilution-only stage during evolution (see Figure 2c, d and e) and post-evolution (Figure 2f) where a return to the original background PND like shape can be seen. Up to 4 evolution sub-stages were observed depending on experimental runs and each sub-stage showed distinct evolution pattern for both particle number and size distributions. These evolution sub-stages are chosen to show pattern of temporal evolution. As is seen in Figures 2b, c, d and e, the shape of normalised PNDs are distinct from each other. Most of the changes occurred during the ‘evolution 1’ stage where the size distributions changed in an unpredictable manner due to rapid dilution induced nucleation. Other evolution sub-stages (2, 3 and 4) show much greater similarity between PNDs taken at every 0.1s; their shape changes in upwards and downwards directions showing a dominance of dilution process. Likewise, post-evolution stage show similar PNDs to those found in pre-evolution stage with a similar pattern of changes in the PND shape without any appreciable change in peak diameters to reflect that these changes are certainly due to dilution.

For covering the entire wake region, on-board measurements were carried out at the points: $x = 0.45$ and 0.90 m; $y = -0.45, 0, 45$; and $z = 0.10, 0.50$ and 0.90 m with respect to x, y and $z = 0$ which are rear end of the car, centre of the car and road level, respectively. Figure 3 shows typical PNCs at $x = 0.45$ m for 30 km h^{-1} speed. Maximum PNCs were recorded, as expected, in line with the tailpipe. The closest measurements points near the tailpipe were at $z = 0.10$ (P_a) and 0.50 m (P_d) above the ground; about up to 2.7 times larger PNCs were recorded at P_a compared with P_d . This can be explained by the fact that P_a is within the direct emission plume while P_d is in flow recirculation zone behind the vehicle. The other characteristics (not shown in Figure 3) were found that PNC increases at P_a with the increase in car speed which is expected due to larger emissions at greater speeds (Kumar et al., 2011) and measurements points are temporally closer at higher speeds. This increase for 30 and 40 km h^{-1} speed is up to 3 times higher than those observed for 20 km h^{-1} . As seen in Figure 3, the PNC decreases with the distance in y -direction while moving away from the tailpipe (i.e. largest in the line with tailpipe $y = -0.45$ and then decreasing at $y = 0$ and 0.45 m).

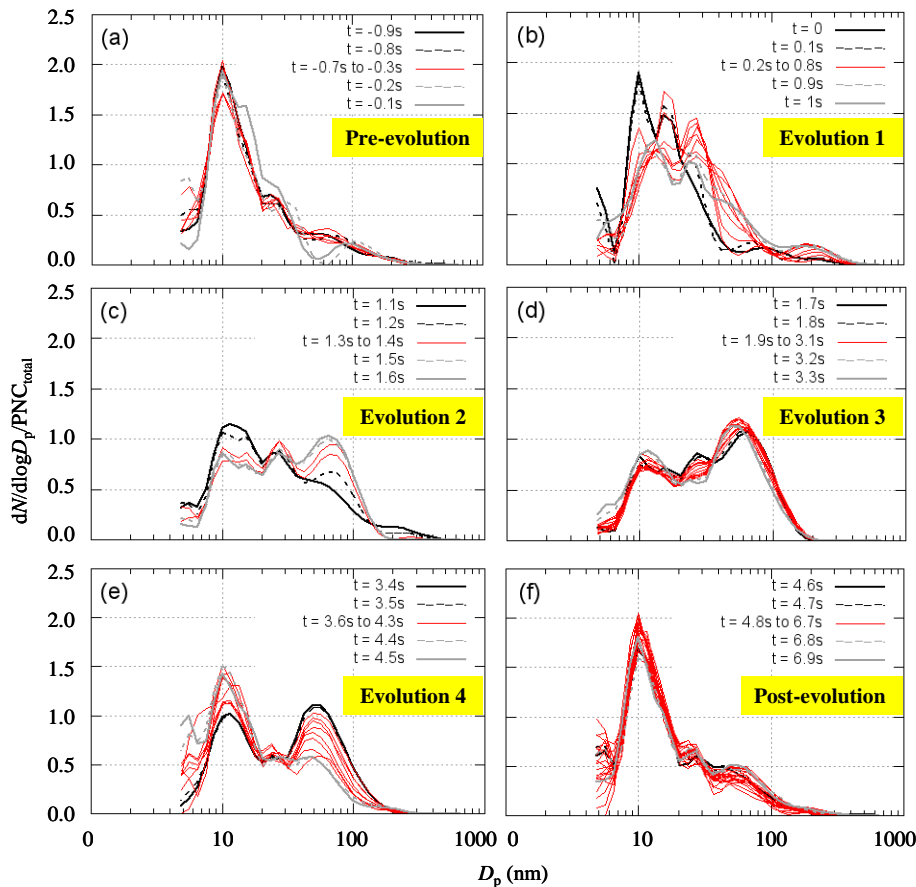


Figure 2. Typical example showing pre-evolution, 4 evolution stages, and post-evolution (experimental case $H = 0.25$ m, $V = 20 \text{ km h}^{-1}$).

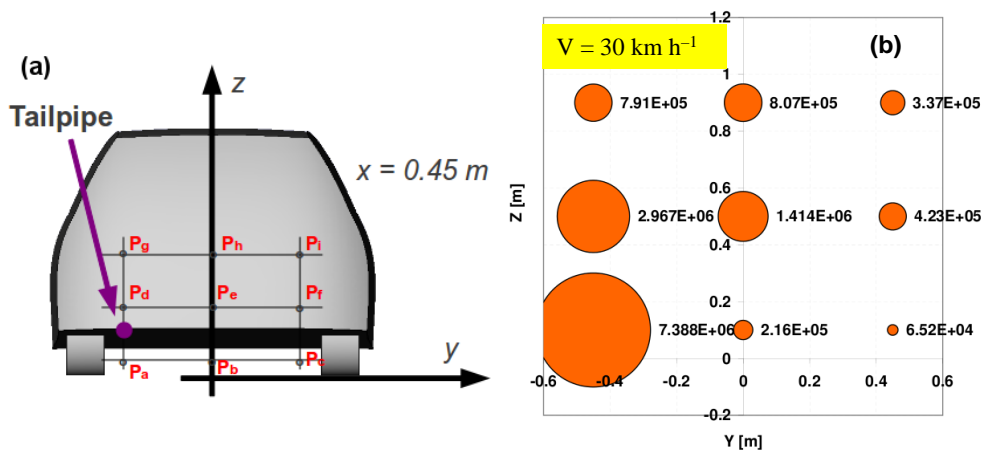


Figure 3. Typical PNCs ($\# \text{ cm}^{-3}$) measured at $x = 0.45$ m during the on-board experiments. Size of each bubble refers to the level of PNCs at an individual point.

Flow and concentration measurements using wind tunnel experiments

Figure 4 shows typical example of vertical cross-sections of wind velocity vectors, root mean square (rms) velocity component in x -direction (u^*) and non-dimensional concentrations ($C^* = CU_{\text{ref}}h^2/Q$) for a 1:5 model; where C is the measured concentrations; U_{ref} is the reference wind speed measured by the ultrasonic anemometers outside the boundary layer; h is the height of the modelled vehicle; Q is the source volumetric flow rate. Velocity and concentration measurements in the wake of the model were measured by LDA and fast FID instruments in a high resolution grid closer to the model (i.e. up to about 5 times the model height) and a relatively larger grid further away from the model.

Figure 4a shows the expected recirculating flow region behind the car; this region has an about $2h$ length. Also can be seen are high speed wind velocities at the lower edge due to the air flow coming from below the car. This recirculation region is also the place where highest longitudinal turbulence can be seen (Figure 4b), particularly near the upper and lower surfaces of the car, which is generated by the flow separation that caused a thin shear layers at both edges. These effects are evident by the concentration measurements shown in Figure 4c. This shows an accumulation of tracer gases within the recirculation region close the rear end the car which is in line with the field measurements (discussed above) where nanoparticles were found to be trapped for a longer time in the recirculation region. Most operational mathematical models often assume classical Gaussian plume dispersion in vehicle wakes but the flow and concentration field demonstrated here shows a different picture. This section only discussed selective result of a 1:5 model but the detailed results can be seen elsewhere (Carpentieri et al., 2011b). Overall, wind tunnel experiments using the other model size (1:20) in the EnFlo tunnel demonstrated similar results and confirmed the development of recirculation zone behind the vehicle, development of plume and dispersion of concentrations within the wake in a nearly similar manner as for 1:5 model.

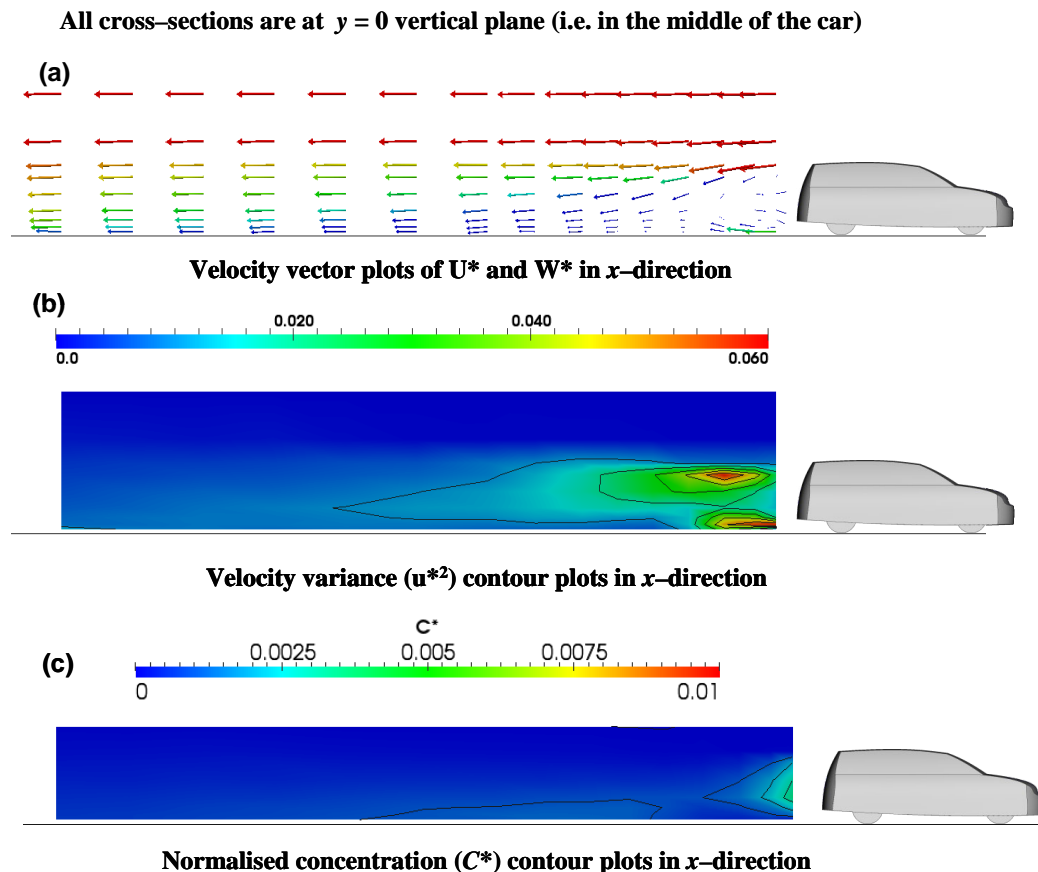


Figure 4. LDA measurements showing (a) velocity vectors, and (b) velocity variances. Fast FID measurements showing (c) concentrations contours. All the results are for a 1:5 model taken at $y = 0$ vertical plane that is at the centre of the vehicle. Both cars and plots are in scale.

Comparison of results from field and wind tunnel measurements

Despite the fact that reduced scale wind tunnel models adopted the same geometrical dimensions of a diesel car that was used for our field measurements (Carpentieri and Kumar, 2011), there were several limitations for making a direct comparison, especially for concentration fields, between the results of both these experiments. This is primarily because measured size resolved distributions of particles during the field study were observed to undergo a range of very fast transformation processes after their release from the tailpipe compared with passive tracer gas used in the wind tunnel which is only affected by dilution. Therefore, a direct comparison of PNCs obtained from both experiments (see, Carpentieri et al., 2011b) indicated an appreciable difference. Especially, the values measured in the field measurements at the closest point to the tailpipe were much greater than those found for wind tunnel measurements. This difference could be attributed to the simplified geometrical details of the vehicle model used in wind tunnel experiments compared with a real car. Furthermore, it was

expected that the tailpipe in the field experiments emitted the plume at the border between the recirculating wake flow and the flow under the car, the tailpipe appeared to emit within the recirculation area in case of wind tunnel model. Emission exit velocity could also have a relevant effect on the concentration distribution in both studies. This paper only highlight very briefly some of the results of this project but more detailed analysis can be found elsewhere (Carpentieri and Kumar, 2011; Carpentieri et al., 2011a, b).

SUMMARY AND CONCLUSIONS

Both the ground-fixed and on-board field measurements using the DMS50 offered an opportunity to measure the number and size distributions of nanoparticles in the near and far wake regions of a moving diesel car. As in our earlier work (Kumar et al., 2009), gathered data was divided into three temporal stages (pre-evolution, evolution and post-evolution). Complex features were found in evolution phase where PNCs and PNDs changed rapidly due to nucleation process driven by dilution. The evolution stage was over within first few seconds. Dilution was found to be the main process affecting the nanoparticle dispersion in near wake where traffic produced turbulence dominates the mixing. Atmospheric turbulence plays a leading role in the far wake region. Effects of dry deposition and coagulation could not be distinguished since the time scales associated with these processes were much larger than the duration of our individual experiments. Integrated results of field measurements indicated the presence of two separate groups of particle in the near wake region: the first being the new particles directly emitted from the tailpipe and the other one being the relatively aged particles which reside in the wake for a longer period by remaining entrained within the recirculation vortices of the vehicle wake. Far wake region contains a mixture of both types of particle groups. These details were often overlooked by past studies. Wind tunnel experiments were carried out to provide detailed assessment of the wake behind the experimental car using reduced scale models in controlled conditions. This part of the study allowed us to characterise the dilution process in the vehicle wake by combining high resolution concentration measurements of a passive tracer gas and three dimensional flow velocity components, and their comparison with the nanoparticle measurements obtained through field study (Carpentieri et al., 2011b). This data also helped to analyse the competing influences and interactions of various transformation processes with each other, providing a solid base for formulating the nanoparticle dispersion model for the vehicle wakes.

ACKNOWLEDGEMENTS

This work has been carried out as a part of the EPSRC grant EP/H026290/1. Dr. Prashant Kumar thankfully acknowledges the receipt of this grant. Authors thank Dr. Paul Hayden, Mr. Allan Wells, Mr. Alastair Reynolds and Mr. Pouyan Joodatnia for their help during experiments.

REFERENCES

- Carpentieri, M. and P. Kumar, 2011: Ground-fixed and on-board measurements of nanoparticles in the wake of a moving vehicle. *Atmospheric Environment*, **in press**, 10.1016/j.atmosenv.2011.1006.1079.
- Carpentieri, M. Kumar, P. and A. Robins, 2011a: An overview of experimental results and dispersion modelling of nanoparticles in the wake of moving vehicles. *Environmental Pollution*, **159**, 685-693.
- Carpentieri, M. Kumar, P. and A. Robins, 2011b: Wind tunnel measurements of flow and dispersion for nanoparticle dispersion modelling in vehicle wakes. *Atmospheric Environment*, ready for submission.
- Kanda, I. Uehara, K. Yamao, Y. Yoshikawa, Y. and T. Morikawa, 2006: A wind-tunnel study on exhaust gas dispersion from road vehicles--Part I: Velocity and concentration fields behind single vehicles. *Journal of Wind Engineering and Industrial Aerodynamics*, **94**, 639-658.
- Kumar, P. Ketzel, M. Vardoulakis, S. Pirjola, L. and R. Britter, 2011: Dynamics and dispersion modelling of nanoparticles from road traffic in the urban atmospheric environment - a review. *Journal of Aerosol Science*, **42**, 580-603.
- Kumar, P. Robins, A. and R. Britter, 2009. Fast response measurements for the dispersion of nanoparticles in a vehicle wake and in a street canyon. *Atmospheric Environment*, **43**, 6110-6118.
- Kumar, P. Robins, A. Vardoulakis, S. and R. Britter, 2010: A review of the characteristics of nanoparticles in the urban atmosphere and the prospects for developing regulatory control. *Atmospheric Environment*, **44**, 5035-5052.